Review

Selective Oxidation of Methane into Methanol Under Mild Conditions

LIU Yifeng[1], WANG Liang[2]✉ and XIAO Feng-Shou[2,3]✉

Received October 25, 2021
Accepted November 30, 2021

Selective oxidation of methane to methanol under mild conditions has been considered as a dream reaction but suffers from poor efficiency due to the strong C—H bond of methane and easy overoxidation of the methanol product. For overcoming these problems, a series of strategies has been developed for improving methanol productivity with oxidants of hydrogen peroxide and even a mixture of oxygen and hydrogen at mild temperatures. Significant achievements in these strategies using effective catalysts, such as supported metal nanoparticles, colloidal metal nanoparticles, and metal@zeolites are briefly concluded. Moreover, the current challenges, future perspectives for preparing active, selective, and stable catalysts, have been discussed. The zeolite fixed metal nanoparticle structure has been found to boost the reaction by benefiting the formation and enrichment of peroxide intermediates, which might guide the development of more efficient catalysts.

Keywords Methane oxidation; Metal@zeolite; Hydrogen peroxide; Methanol

1 Introduction

Methane, one of the most important carbon resources, has huge reserves on the earth. The energy-consuming conventional route to its industrial application requires reforming of methane to syngas, followed by further conversion to methanol because methanol[1—5] acts as a platform to produce olefins, aromatics, and many building blocks for the production of fine chemicals[6—10]. Compared with such a non-direct route, direct partial oxidation of methane into methanol has been paid much attention, but it still has a challenge because of the strong C—H bond(104 kcal/mol, 1cal=4.18 J) with negligible electron affinity, causing the difficulty in C—H activation under mild conditions[11—15]. As well, the methanol product is more active than methane, giving overoxidation to form valueless CO_2. To get over these shortcomings, relatively expensive and toxic oxidants have been employed for methane oxidation[16—20]. For example, strongly acidic oleum could react with methane to obtain methyl bisulfate over a Hg or Pt catalyst, then methanol was obtained *via* subsequent hydrolysis that also forms stoichiometric SO_2. In addition, cationic Au and Pt catalysts could also catalyze the methane oxidation, but strong oxidizing agents(*e.g.*, selenic acid) were required, producing environmentally unfriendly by-products.

The metal-exchanged zeolite catalysts could catalyze the methane oxidation using oxygen or even water, which efficiently inhibited the methanol overoxidation[21—28], but still required high temperatures(200—500 °C) for the intermittent steps to activate the metal sites, oxidize methane, and desorb the methanol product.

Facing the aforementioned challenges, the environmentally benign oxidant of hydrogen peroxide(H_2O_2) has significant advantages in methane oxidation without any toxic salts or strong acids[29—33]. Great attention has been focused in this route to develop multiple catalysts, where various oxygenates were obtained. The heteroatom zeolites (*e.g.*, Fe-ZSM-5) could efficiently catalyze the methane oxidation using H_2O_2, where formic acid was a dominant product. Higher methanol selectivity could be obtained with colloidal metal nanoparticles(AuPd colloid).

Further exploration was performed in the direct synthesis of H_2O_2 from gaseous H_2 and O_2, and then the methane was oxidized. Notably, the supported metal nanoparticle catalysts surfer from poor efficiency with a very small amount of methanol products because of the insufficient concentration of hydrogen peroxide compared with that directly using H_2O_2. Successes were obtained using the AuPd nanoparticles fixed within zeolite crystals that were hydrophobilized on the external surface, which highly enriched the hydrogen peroxide *via* a so-called molecular-fence effect to improve the methanol yield.

Currently, the conversion of methane *via* oxidative and non-oxidative routes under harsh conditions over different catalysts has been summarized[34,35], but methane oxidation under mild conditions has been rarely discussed. Herein,

✉ XIAO Feng-Shou
fsxiao@zju.edu.cn
✉ WANG Liang
liangwang@zju.edu.cn
1. Key Lab of Applied Chemistry of Zhejiang Province, Department of Chemistry, Zhejiang University, Hangzhou 310028, P. R. China;
2. Key Lab of Biomass Chemical Engineering of Ministry of Education, College of Chemical and Biological Engineering, Zhejiang University, Hangzhou 310027, P. R. China;
3. Zhejiang Tianlan Environmental Protection Technology Limited Company, Hangzhou 310012, P. R. China

https://doi.org/10.1007/s40242-022-1428-z

we focus on synthesizing effective catalysts and designing novel strategies for methane oxidation using H_2O_2(pre-introduced and *in-situ* synthesis) as an oxidant, which is helpful for guiding the efficient utilization of methane(Table 1).

Table 1 Performances of various catalysts for methane oxidation under mild conditions

Entry	Catalyst	*T*/°C	Oxidant	Amount of products/μmol			Amount of Total prod.	CH_3OH sel.(%)	CH_4 conv.(%)	Ref.
				CH_3OH	MeOOH	HCOOH				
1	2.5%Fe/ZSM-5	50	0.5 mol/L H_2O_2	22.3	1.8	164.0	—	12	0.7	[32]
2	Cu-2.5%Fe/ZSM-5	50	0.5 mol/L H_2O_2	188.8	0.5	0	—	85	0.7	[32]
3	0.5%Fe-silicalite-1	70	1.0 mol/L H_2O_2	15.1	10.2	156.7	—	8	10.5	[32]
4	0.5%Fe-silicalite-1 and Cu/silicalite-1	70	1.0 mol/L H_2O_2	168.4	0	0	—	93	10.1	[32]
5	1.0%AuPd/TiO_2	70	0.5 mol/L H_2O_2	0.66	3.90	0	1.03[a]	12.9	—	[3]
6	5.0%AuPd/TiO_2	70	0.86%H_2/1.72%O_2	0.81	0.1	0	0.06[a]	79.4	—	[3]
7	5.0%AuPd/TiO_2	50	0.009%NADH/0.002%O_2	4.48	0	0	0.08[a]	89.2	—	[3]
8	Au-Pd colloid	50	1000 μmol H_2O_2	3.3	11.8	0.6	29.4[a]	—	—	[2]
9	Au-Pd colloid	50	1000 μmol H_2O_2/5 bar O_2	7.6	17.4	1.8	53.6[a]	—	—	[2]
10	Au-Pd colloid	50	50 μmol H_2O_2/5 bar O_2	2.8	15.7	1.2	39.4[a]	—	—	[2]
11	AuPd@ZSM-5	70	0.03%H_2/0.06% O_2	23.0	Trace	Trace	32.9[b]	—	—	[36]
12	AuPd/ZSM-5	70	0.03%H_2/0.06 %O_2	7.1	Trace	Trace	10.1[b]	—	—	[36]
13	AuPd@ZSM-5-C_{16}	70	0.03%H_2/0.06 %O_2	64.1	Trace	Trace	91.6[b]	92.0	17.3	[36]

a. Total prod.(mol·kg_{cat}^{-1}·h^{-1}); *b*. total prod.(mol·kg_{AuPd}^{-1}·h^{-1}).

2 Selective Methane Oxidation with H_2O_2

In the previous study in methane oxidation using a net reaction[1], the C—H bond was activated by SO_3 and H_2SO_4, then the obtained CH_3OSO_3H was hydrated to produce methanol and H_2SO_4. In this case, the homogeneous (bpym)$PtCl_2$ catalyst was employed, which has a challenge in the catalyst separation and regeneration.

H_2O_2 is an environmentally friendly oxidant because its by-product is only water. With the employment of H_2O_2, several traditional chemical oxidation processes with heavy pollution have been changed into sustainable ones, such as propene epoxidation, ketone ammoxidation, and benzene hydroxylation. Following this trend, hydrogen peroxide was employed in methane oxidation. Hutchings and co-workers[32] obtained methyl hydroperoxide(CH_3OOH), CH_3OH, and formic acid(HCOOH) products using H_2O_2 over a Fe^{2+}-exchanged ZSM-5 zeolite in aqueous media at 50 °C. Fe-silicalite-1 showed higher activity, with a 10% conversion with 96% selectivity to oxygenated products(CH_3OH, CH_3OOH, HCOOH). Introducing Cu^{2+} to the reaction intensively hindered the over-oxidation process, and the methanol selectivity could reach as high as 85%. Through several alternative model structures, the closed match was obtained for a di-iron complex $[Fe_2(\mu_2\text{-}OH)^2(OH)^2(H^2O)^2]^{2+}$, containing an antiferromagnetically coupled high-spin octahedral Fe^{3+} center, which represented the resting state of the active site in the catalyst. DFT calculations were used to understand a molecular level mechanism for methane oxidation(Fig.1). Within this proposed cycle, the di-iron site **1** first coordinates H_2O_2 through exchange with a water ligand to give species **2**. H^+-transfer and solvent rearrangement then forms species **3**, which is formally an Fe^{4+}/Fe^{2+} dimer. A second H_2O/H_2O_2 exchange occurs for H_2O_2 at the Fe^{2+} site, although the H_2O_2 cannot give a second surface hydroperoxide because there is no adjacent ligand that can easily abstract H^+. They proposed similar event here to generate species **4**. In contrast to the isolated Fe^{4+}═O sites, the formation of an Fe^{4+}═O species adjacent to Fe-OOH results in a bifunctional oxidation center (species **4** in Fig.1), which is favorable for the methane activation process.

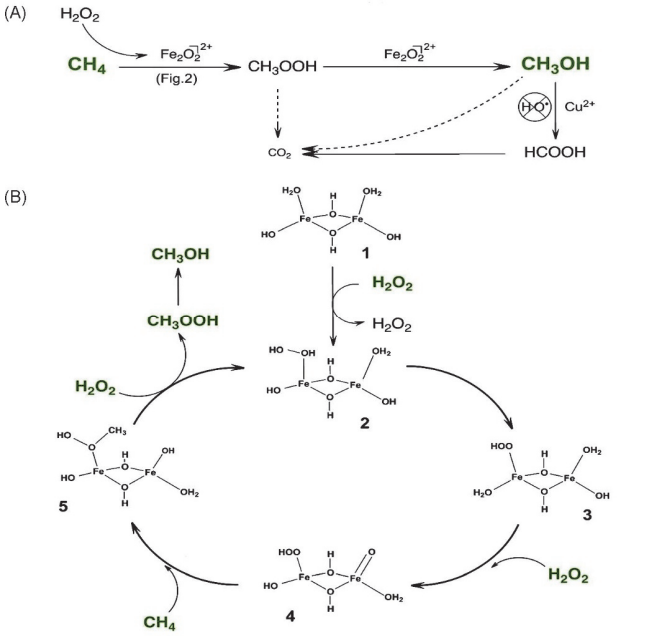

Fig.1 Potential reaction scheme for the methane oxidation based on the time-on-line profile(A) and catalytic cycle for the oxidation of methane to CH_3OOH using H_2O_2, catalysed by a binuclear Fe species in ZSM-5(B)

Reproduced with permission from Ref.[32], Copyright 2012, Wildy-VCH.

https://doi.org/10.1007/s40242-022-1428-z

In this process, hydrogen peroxide reacted with the Fe centres for the activation of the carbon-hydrogen bond, forming methyl hydroperoxide as the primary product. While Cu species did not play a direct role in methane activation, it facilitated the formation of methanol by inhibiting over oxidation to formic acid and CO_2. Adding Cu species to the reaction system, either as a component of the heterogeneous catalyst or as a heterogeneous or homogeneous additive to the reaction mixture, could drastically reduce the over-oxidation product selectivity(*e.g.*, formic acid), and improve the methanol selectivity. This phenomenon is due to that the Cu species could reduce the hydroxyl radicals in the reaction system, which has been regarded as a crucial factor for the overoxidation to form formic acid, as confirmed by the electron paramagnetic resonance(EPR) study[32].

The reaction mechanism is sensitive to the structure of Fe sites. For example, Deng and co-workers[37] reported different active sites of O-FeN_4-O, where H_2O_2 molecules were absorbed and decomposed into H_2O and an adsorbed O atom for the subsequent methane oxidation steps. In this case, the by-product of $HOCH_2OOH$ was observed, while it was undetectable in the oxidation using the Fe-zeolite catalyst.

In the reaction with H_2O_2, inhibiting H_2O_2 decomposition and hydrogenation is essential. Hutchings and co-workers[3] reported 1%(mass fraction) AuPd/TiO_2 prepared by incipient wetness is active for the oxidation of methane with low rates for H_2O_2 decomposition and hydrogenation. After enhancing metal loading to 5%(mass fraction), catalyst gave a higher methanol selectivity than the 1%(mass fraction) AuPd/TiO_2 catalyst, but a similar overall oxygenate selectivity. Using H_2O_2 in methane oxidation could get the stoichiometric ideal product, but the utilization rate of H_2O_2 and the oxygenate selectivity are still low. The most significant differences between the methane oxidation using H_2O_2 over AuPd-based and Fe-ZSM-5 catalysts are the reaction intermediate of $^{\bullet}CH_3$ radical. Methane oxidation on supported Au-Pd nanoparticles involves $^{\bullet}CH_3$ radical formation as confirmed by EPR[3]. However, in the methane oxidation using Fe-ZSM-5, $^{\bullet}CH_3$ radical was undetectable.

3 Partial Oxidation of Methane with H_2O_2 and Oxygen

Although oxygenated products(CH_3OH, CH_3OOH, HCOOH) could be obtained with H_2O_2 as an oxidant, the high cost of H_2O_2 is difficult for practical applications of methane oxidation. Relative to H_2O_2, gaseous oxygen is much cheap. Hutchings and co-workers[2] showed the partial oxidation of methane into methanol under mild conditions using colloidal Au-Pd NPs in the presence of both H_2O_2 and O_2. In this reaction, possible intermediates are methyl($^{\bullet}CH_3$) and hydroxyl($^{\bullet}OH$) radicals, as evidenced by EPR spectroscopy[3,38]. In addition, the observation of CH_3OOH in the reaction implies that the primary termination is either between $^{\bullet}CH_3$ and $^{\bullet}OOH$ radicals or from recombination of $^{\bullet}CH_3$ with dissolved O_2 in the solution resulted from the decomposition of H_2O_2.

With isotopic labelling research, the initial activation of CH_4 to $^{\bullet}CH_3$ is suggested from a radical mechanism(Fig.2), where $^{\bullet}CH_3$ radicals can react directly with dissolved O_2. Several products containing ^{16}O were obtained through radical reactions between $^{\bullet}CH_3$ with either $^{\bullet}{}^{16}O{}^{16}OH$ or $^{16}O_2$, which were generated from the decomposition of $H_2{}^{16}O_2$. The $^{\bullet}CH_3$ radicals were formed *via* hydrogen abstraction by $^{\bullet}OH$ from H_2O_2, which activated CH_4. In the ideal reaction, 10 μmol of H_2O_2 and 5 bar(5×10^5 Pa) of $^{18}O_2$ pressure were required to generate 20 μmol of oxygenate products, which contained 70% ^{18}O and 30% ^{16}O. These isotopic ratios and the reaction scheme proposed were broadly in line, where 10 μmol were used to generate $^{\bullet}CH_3$ radicals and 6 μmol were used in ^{16}O products *via* decomposition. Higher efficiency was achieved by using H_2O_2 to activate CH_4 with O_2 rather than supply oxygen into the primary products.

To investigate whether $^{\bullet}OH$ could activate methane, Fe-based Fenton catalyst with H_2O_2 was tested, giving little methanol products. These results indicate that AuPd colloidal nanoparticles are also essential for CH_4 activation. Meanwhile, it could be desirable to couple the Au-Pd colloidal catalyst with a photochemical[39,40] or electrochemical fuel cell[41,42] to generate $^{\bullet}OH$ for H abstraction to facilitate $^{\bullet}CH_3$ radical formation rather than using H_2O_2.

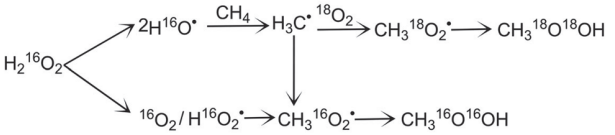

Fig.2 Proposed reaction scheme for methane oxidation in the presence of H_2O_2 and molecular O_2

Reproduced with permission from Ref.[2], Copyright 2017, American Association for the Advancement of Science.

4 Methane Oxidation with O_2 and H_2

It has been reported that a soluble co-reductant, reduced nicotinamide adenine dinucleotide, with AuPd catalyst and O_2 were used for methane oxidation, and micromolar methanol was observed. This work suggests that the use of other reductants is possible. Therefore, Hutchings and co-workers[3] performed reactions using CH_4, H_2, and O_2 diluted with N_2(0.86% of H_2 and 1.72% of O_2 in the reactor gas feed) for concurrent synthesis of *in-situ* hydrogen peroxide and eventual formation of methanol. Compared with using H_2O_2, similar productivity but improved methanol selectivity were found in the presence of O_2 and H_2. However, the total product

https://doi.org/10.1007/s40242-022-1428-z

is still insufficient. This phenomenon might be related to a relatively low H_2O_2 concentration near the catalytically active nanoparticles[43], where the key intermediate of H_2O_2 generated from H_2 and O_2 can readily diffuse away from the active sites.

Based on this hypothesis, it is suggested that preventing H_2O_2 dilution and thereby keeping a high local concentration of H_2O_2 around the active site could promote methane conversion.

Recently, Xiao and co-workers[36] proposed a molecular-fence concept, showing a heterogeneous catalyst for enhanced methanol productivity in methane oxidation by *in-situ* generated hydrogen peroxide at the mild temperature (70 °C). A series of catalysts, encapsulating AuPd alloy nanoparticles in zeolite crystals, could efficiently generate H_2O_2 with H_2 and O_2 and then oxidize methane into methanol. With primary experience, they designed a series AuPd@zeolite-R catalysts, in which AuPd alloy nanoparticles were fixed in aluminosilicate zeolite crystals, followed by hydrophobization that rendered the external surface of the zeolite hydrophobic by appending organosilanes(R), as given in Fig.3. The organosilanes contributed to allowing hydrogen, oxygen, and methane to diffuse to the catalytically active sites quickly to form H_2O_2 in the zeolite. Once the hydrophobic sheath was ready, the generated H_2O_2 was difficult for diffusing out of the zeolite crystals, raising its concentration in the zeolite crystals. At the same time, the hydrophobic methane molecules could efficiently pass through the hydrophobic sheath to access the AuPd nanoparticles. As a result, 17.3% conversion of methane and 92% selectivity for methanol were observed. The productivity of methanol reached 91.6 millimoles per gram of AuPd per hour, as shown in Fig.4. Compared with previous catalysts, the AuPd@zeolite-R showed remarkable superiority on methane oxidation because of its high activity and cheap mixture of hydrogen and oxygen. However, the productivity of methane is still lower than that of direct use of H_2O_2, which might be related to the efficiency for the formation of H_2O_2 from H_2 and O_2. Therefore, studies on the direct synthesis of H_2O_2 from H_2 and O_2 should be carefully investigated.

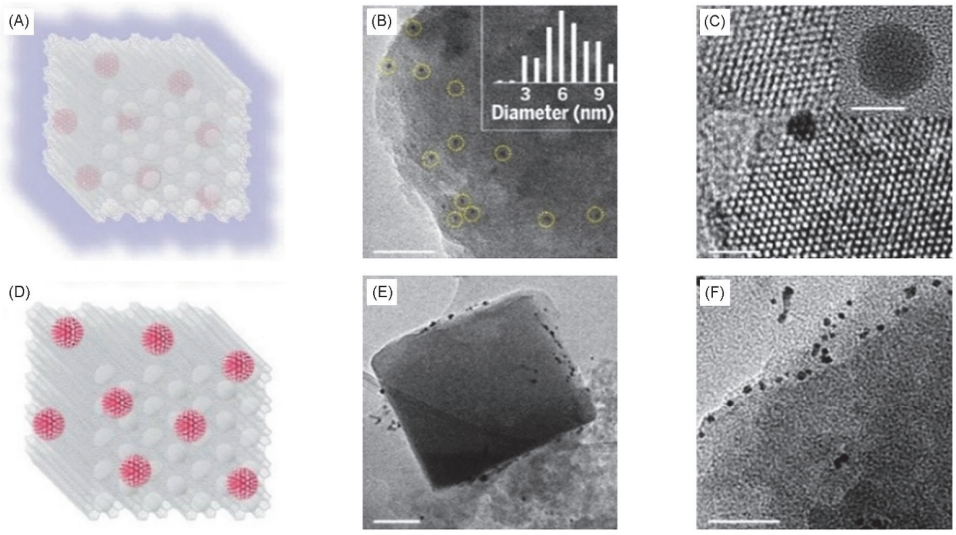

Fig.3 Models and tomographic section TEM images of AuPd@ZSM-5-C_{16}(A—C) and AuPd/ZSM-5(D—F)

Scale bars: (B) 100 nm, (C) 10 nm(5 nm in inset), (E) 200 nm, (F) 50 nm. Reproduced with permission from Ref.[36], Copyright 2020, American Association for the Advancement of Science.

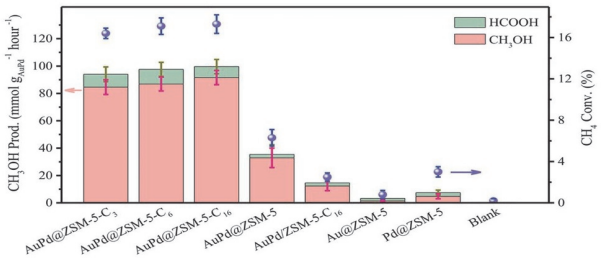

Fig.4 Data characterizing the oxidation of methane with H_2 and O_2 over various catalysts

Reproduced with permission from Ref.[36], Copyright 2020, American Association for the Advancement of Science.

5 Direct Synthesis of H_2O_2

There are many successful examples for direct synthesis of H_2O_2 from H_2 and O_2. Hutchings *et al.*[44] showed selectivity of >95% toward H_2O_2 over palladium catalysts by adding the second metal oxide to Pd oxide supported on titania. Huang *et al.*[45] reported a series of PdSn bimetallic nanocrystals with hollow structures, which were highly active and selectives, where H_2O_2 decomposition and hydrogenation were completely inhibited. When water was employed as the solvent, excellent activity(120.1 $mol \cdot kg_{cat}^{-1} \cdot h^{-1}$) could be

https://doi.org/10.1007/s40242-022-1428-z

achieved.

Xiao and co-workers[46] found that AuPd nanoparticles within the aluminosilicate zeolite crystals(AuPd@HZSM-5) can catalyze the oxygen hydrogenation to form H_2O_2 by a zeolite-assisted proton transfer process. The protons also stabilized the H_2O_2 product and reduced H_2O_2 decomposition. The H_2O_2 productivity could reach 320 mmol·g_{AuPd}^{-1}·h^{-1} with a H_2 selectivity of 88% in water, showing great advances compared with the conventionally supported metal nanoparticle catalysts. Due to using water as a solvent, the formed H_2O_2 aqueous solution can be directly used in the Fenton system for pollutant removal in environmental protection. This work deepens the structure performance understanding of catalysts for H_2O_2 synthesis, which might offer an alternative way for the rational design of more efficient catalysts.

Other fancy strategies have been explored to produce H_2O_2 from electrochemical routes. Wang and his co-workers[47] designed an electrosynthesis system to generate high concentration of H_2O_2, and achieved over 90% selectivity for pure H_2O_2 at current densities up to 200 milliamperes per square centimetre. The concentration of pure H_2O_2 solutions could be obtained up to 20%(mass fraction). Moreover, through control of oxygen reduction pathways on different transition metal single-atom coordination in a carbon nanotube, their group found Fe-C-O as an efficient H_2O_2 catalyst, with an unprecedented onset of 0.822 V *versus* a reversible hydrogen electrode in 0.1 mol/L KOH to deliver 0.1 mA/cm^2 H_2O_2 current, and the selectivity could reach 95% in both alkaline and neutral media[48]. These successful works have great importance for the rational design of highly efficient catalysts for on-purpose H_2O_2 technologies.

6 Summary and Outlook

In summary, this minireview briefly summarized developments for selective oxidation of methane, where H_2O_2 synthesized *in-situ* from hydrogen and oxygen was selected as an ideal oxidant. In addition, fixed metal alloy nanoparticles inside the zeolite crystals with hydrophobic surfaces combined the advantages of both highly active sites and high concentration of H_2O_2 oxidant, where the radical mechanism was simply discussed.

Based on the current understanding, great efforts are still required for overcoming the challenges of methane oxidation. Future works could focus on designing effective catalysts and regulating metal nanoparticles sizes. Besides conventional supports, such as TiO_2, other modified supports such as zeolites could be employed in methane oxidation. Furthermore, the surface of zeolite could be modified, such as hydrophobic coating as molecular-fence to allow the diffusion of hydrogen, oxygen, and methane to the catalyst active sites, while the generated hydrogen peroxide was remained inside the zeolite crystals for the conversion of methane into methanol.

In addition, the mechanism of partial methane oxidation should be further explored. With a full understanding of methane oxidation pathway, we can design highly active catalysts that match with the reaction. Assisted by computational chemistry and artificial intelligence, the methane oxidation pathway might be calculated and simulated. Further understanding on the reaction mechanism is critical for the preparation of highly efficient catalysts in the future.

Acknowledgements

This work was supported by the National Natural Science Foundation of China (No.21932006).

Conflicts of Interest

The authors declare no conflicts of interest.

References

[1] Periana R. A., Taube D. J., Gamble S., Taube H., Satoh T., Fujii H., *Science*, **1998**, *280*, 560
[2] Agarwal N., Freakley S. J., McVicker R. U., Althahban S. M., Dimitratos N., He Q., Morgan D. J., Jenkins R. L., Willock D. J., Taylor S. H., Kiely C. J., Hutchings G. J., *Science*, **2017**, *358*, 223
[3] Ab Rahim M. H., Forde M. M., Jenkins R. L., Hammond C., He Q., Dimitratos N., Lopez-Sanchez J. A., Carley A. F., Taylor S. H., Willock D. J., Murphy D. M., Kiely C. J., Hutchings G. J., *Angew. Chem. Int. Ed.*, **2013**, *52*, 1280
[4] Palkovits R., Antonietti M., Kuhn P., Thomas A., Schüth F., *Angew. Chem. Int. Ed.*, **2009**, *48*, 6909
[5] Saha D., Grappe H. A., Chakraborty A., Orkoulas G., *Chem. Rev.*, **2016**, *116*, 11436
[6] Schwach P., Pan X., Bao X., *Chem. Rev.*, **2017**, *117*, 8497
[7] Svelle U. S., Bjørgen M., Beato P., Janssens T. V. W., Joensen F., Bordiga S., Lillerud K. P., *Angew. Chem. Int. Ed.*, **2012**, *51*, 5810
[8] Guo X., Fang G., Li G., Ma H., Fan H., Yu L., Ma C., Wu X., Deng D., Wei M., Tan D., Si R., Zhang S., Li J., Sun L., Tang Z., Pan X., Bao X., *Science*, **2014**, *344*, 616
[9] Cope´ret C., *Chem. Rev.*, **2010**, *110*, 656
[10] Cui Z.-M., Liu Q., Song W. G., Wan L. J., *Angew. Chem. Int. Ed.*, **2006**, *45*, 6512
[11] Balasubramanian R., Smith S. M., Rawat S., Yatsunyk L. A., Stemmler T. L., Rosenzweig A. C., *Nature*, **2010**, *465*, 115
[12] Ahlquist M., Nielsen R. J., Periana R. A., Goddard 3rd W. A., *J. Am. Chem. Soc.*, **2009**, *131*, 17110
[13] Lunsford J. H., *Catal. Today*, **2000**, *63*, 165
[14] Luk H. T., Mondelli C., Ferré D. C., Stewart J. A., Pérez-Ramírez J., *Chem. Soc. Rev.*, **2017**, *46*, 1358
[15] Martin O., Martn A. J., Mondelli C., Mitchell S., Segawa T. F., Hauert R., Drouilly C., Curulla-Ferré D., Prez-Ramrez J., *Angew. Chem. Int. Ed.*, **2016**, *55*, 6261
[16] Centi G., Perathoner S., *Catalysis Today*, **2009**, *148*, 191
[17] Roudesly F., Oble J., Poli G., *J. Mol. Catal. Chem.*, **2017**, *426*, 275
[18] Morejudo S. H., Zanón R., Escolástico S., Yuste-Tirados I., Malerød-Fjeld H., Vestre P. K., W. G. Coors W. G., Martínez A., Norby T.,. Serra J. M., Kjølseth C., *Science*, **2016**, *353*, 563
[19] Lieberman R. L., Rosenzweig A. C., *Nature*, **2005**, *434*, 177
[20] Periana R. A., Mironov O., Taube D., Bhalla G., Jones C. J., *Science*, **2003**, *301*, 814
[21] Natte K., Neumann H., Beller M., Jagadeesh R. V., *Angew. Chem. Int. Ed.*, **2017**, *56*, 6384
[22] Schröder D., Schwarz H., *Proc. Natl. Acad. Sci. USA*, **2008**, *105*, 18114
[23] Schroeder D., Fiedler A., Hrusak J., Schwarz H., *J. Am. Chem. Soc.*, **1992**, *114*, 1215
[24] Sushkevich V. L., Palagin D., Ranocchiari M., van Bokhoven J. A., *Science*, **2017**, *356*, 523

[25] Groothaert M. H., Smeets P. J., Sels B. F., Jacobs P. A., Schoonheydt R. A., *J. Am. Chem. Soc.*, **2005**, *127*, 1394
[26] Smeets P. J., Groothaert M. H., Schoonheydt R. A., *Catal. Today*, **2005**, *110*, 303
[27] Woertink J. S., Smeets P. J., Groothaert M. H., Vance M. A., Sels B. F., Schoonheydt R. A., Solomona E. I., *Proc. Natl. Acad. Sci. USA*, **2009**, *106*, 18908
[28] Alayon E. M., Nachtegaal M., Ranocchiari M., van Bokhoven J. A., *Chem. Commun.*, **2012**, *48*, 404
[29] Tomkins P., Ranocchiari M., van Bokhoven J. A., *Acc. Chem. Res.*, **2017**, *50*, 418
[30] Cui X., Wang Y., Hu Y., Hua L., Li H., Han X., Liu Q., Yang F., He L., Chen X., Li Q., Xiao J., Deng D., Bao X., *Chem*, **2018**, *4*, 1902
[31] Huang W., Zhang S., Tang Y., Li Y., Nguyen L., Li Y., Shan J., Xiao D., Gagne R., Frenkel A. I., Tao F.(Feng), *Angew. Chem. Int. Ed.*, **2016**, *55*, 13441
[32] Hammond C., Forde M. M., Ab Rahim M. H., Thetford A., He Q., Jenkins R.t L., Dimitratos N., Lopez-Sanchez J. A., Dummer N. F., Murphy D. M., Carley A. F., Taylor S. H., Willock D. J., Stangland E. E., Kang J., Hagen H., Kiely C. J., Hutchings G. J., *Angew. Chem. Int. Ed.*, **2012**, *124*, 5219
[33] Grundner S., Markovits M. A.C., Li G., Tromp M., Pidko E. A., Hensen E. J. M., Jentys A., Sanchez-Sanchez M., Lercher J. A., *Nat. Commun.*, **2015**, *6*, 7546
[34] Liu Y., Deng D., Bao X., *Chem*, **2020**, *10*, 2497
[35] Zhang Q., Yu J., Corma A., *Adv. Mater.*, **2020**, *32*, 2002927
[36] Jin Z., Wang L., Zuidema E., Mondal K., Zhang M., Zhang J., Wang C., Meng X., Yang H., Mesters C., Xiao F.-S., *Science*, **2020**, *367*, 193
[37] Cui X., Li H., Wang Y., Hu Y., Hua L., Li H., Han X., Liu Q., Yang F., He L., Chen X., Li Q., Xiao J., Deng D., Bao X., *Chem.* **2018**, 4, 1902
[38] Xie J., Yu J., Rudolph M., Rominger F., Hashmi A. S. K., *Angew. Chem. Int. Ed.*, **2016**, *55*, 9416
[39] Noceti R. P., Taylor C. E., D'Este J. R., *Catal. Today*, **1997**, *33*, 199
[40] Gondal M. A., Hameed A., Suwaiyan A., *Appl. Catal. A Gen.*, **2003**, *243*, 165
[41] Frese Jr. K. W., *Langmuir*, **1991**, *7*, 13
[42] Tomita A., Nakajima J., Hibino T., *Angew. Chem. Int. Ed.*, **2008**, *47*, 1462
[43] Xie J., Jin R., Li A., Bi Y., Ruan Q., Deng Y., Zhang Y., Yao S., Sankar G., Ma D., Tang J., *Nat. Catal.*, **2018**, *1*, 889
[44] Freakley S. J., He Q., Harrhy J. H., Lu L., Crole D. A., Morgan D. J., Ntainjua E. N., Edwards J. K., Carley A. F., Borisevich A. Y., Kiely C. J., Hutchings G. J., *Science*, **2016**, *351*, 965
[45] Li F., Shao Q., Hu M., Chen Y., Huang X., *ACS Catalysis*, **2018**, *8*, 3418
[46] Jin Z., Liu Y., Wang L., Wang C., Wu Z., Zhu Q., Wang L., Xiao F.-S., *ACS Catalysis*, **2021**, *11*, 1946
[47] Xia C., Xia Y., Zhu P., Fan L., Wang H., *Science*, **2019**, *366*, 226
[48] Jiang K., Back S., Akey A. J., Xia C., Hu Y., Liang W., Schaak D., Stavitski E., Nørskov J. K., Siahrostami S., Wang H., *Nat. Commun.*, **2019**, *10*, 39